Crystal structure and low-temperature magnetic properties of $R_mM\mathrm{In}_{3m+2}$ compounds (M=Rh or Ir; m=1,2; R=Sm or Gd)

P. G. Pagliuso, J. D. Thompson, M. F. Hundley, J. L. Sarrao, and Z. Fisk*
Los Alamos National Laboratory, Los Alamos, New Mexico 87545
(Received 29 August 2000; published 11 January 2001)

We have synthesized the series of compounds $RM\mathrm{In}_5$ and $R_2M\mathrm{In}_8$ in single crystal form, where R=Sm or Gd and M=Rh or Ir. These materials form in tetragonal derivatives of the Cu_3Au structure $R\mathrm{In}_3$. Measurements of magnetic susceptibility, electrical resistivity, and low-temperature heat capacity are reported. These compounds order antiferromagnetically at low temperature (T_N<45 K) and their low-temperature magnetic properties remain nearly unaltered compared to their $SmIn_3$ and $GdIn_3$ cubic relatives. The present data are compared to the magnetic properties of the isostructural (Ce,Nd) (Rh,Ir)In_5 and $(Ce,Nd)_2(Rh,Ir)\mathrm{In}_8$ compounds, and the validity of de Gennes scaling as a function of rare earth in a given structure is discussed.

DOI: 10.1103/PhysRevB.63.054426 PACS number(s): 75.50.Ee, 75.30.Gw, 75.10.Dg, 75.20.En

I. INTRODUCTION

Recently, a new series of $R_mM\mathrm{In}_{3m+2}$ tetragonal variants of the Cu_3Au-structure compounds for M=Rh or Ir, m=1,2; and R=light rare earth have become a particularly relevant area of research since the discovery of a new class of heavy-fermion superconductors for some of the Ce-based compounds.[1–3] The $R_mM\mathrm{In}_{3m+2}$ tetragonal structures can be viewed as m layers of $R\mathrm{In}_3$ units stacked sequentially along the c axis with intervening layers of $M\mathrm{In}_2$ (Ref. 4) and unconventional magnetic and superconducting behavior have been reported for $CeRhIn_5$ (Ref. 1) and $CeIrIn_5$.[2] The first one is an antiferromagnet at ambient pressure ($T_N\approx3.8$ K and $\gamma\approx400$ mJ/mol K^2),[1] and presents an unconventional evolution to a superconducting state for $P>P_c\approx16$ kbars where superconductivity sets in at $T_c\approx2$ K. $CeIrIn_5$ shows ambient-pressure heavy-fermion superconductivity at $T_c\approx0.4$ K with a Sommerfeld coefficient of $\gamma\approx720$ mJ/mol K^2.[2] The m=2 variants of these Ce-based compounds include an antiferromagnetic ground state ($T_N\approx2.8$ K and $\gamma\approx400$ mJ/mol K^2) for Ce_2RhIn_8, while Ce_2IrIn_8 remains a heavy-fermion paramagnet to 50 mK, with no evidence for a phase transition ($\gamma\approx700$ mJ/mol K^2).[3]

It has been suggested that the reduced spatial dimensionality and magnetic anisotropy resulting from the quasi-two-dimensional structure of these compounds may control the nature of their heavy-fermion ground states.[1,3] Furthermore, studies of $Nd\mathrm{In}_5$ and $Nd_2M\mathrm{In}_8$ analogs for M=Rh or Ir suggest that crystal-field effects (CEF's) and related magnetic anisotropy play an important role in the evolution of the magnetic properties within these series.[5] Therefore studies of the magnetic properties through the rare earths for $R_mM_n\mathrm{In}_{3m+2n}$ (M=Rh or Ir) appear to be a promising investigation. The Pr-based homologues are nonmagnetic singlet ground-state systems and a detailed CEF analysis of these materials will be given elsewhere.[6]

In the present work, we report magnetic susceptibility, electrical resistivity, and heat-capacity measurements on $(Gd,Sm)M\mathrm{In}_5$ and $(Gd,Sm)_2M\mathrm{In}_8$ single crystals, for M=Rh or Ir. Each orders antiferromagnetically with $T_N\lesssim45$ K. Comparisons to their cubic relative $(Gd,Sm)\mathrm{In}_3$ suggest that the insertion of $M\mathrm{In}_2$ layers along the c axis in $(Gd,Sm)M\mathrm{In}_5$ and $(Gd,Sm)_2M\mathrm{In}_8$ (M=Rh or Ir) only weakly affects the low-temperature magnetic ground state for the tetragonal variants. The data for the Ce and Nd-based homologues are also included to help the discussion.

II. EXPERIMENT

Single crystalline samples of the $(Gd,Sm)M\mathrm{In}_5$ and $(Gd,Sm)_2M\mathrm{In}_8$ (M=Rh or Ir) compounds were grown from the melt in In flux as described previously.[1] Typical crystal sizes were 1×1 cm×several mm. The tetragonal $HoCoGa_5$ (m=1) (Ref. 4) and Ho_2CoGa_8 (m=2) (Ref. 7) structure types and phase purity were confirmed by x-ray powder diffraction, and the crystal orientation was determined by the usual Laue method. The lattice parameters a and c for the studied compounds are given in Table I. Lattice constants for the nonmagnetic variants $LaM\mathrm{In}_5$ and $La_2M\mathrm{In}_8$ are also included for reference. Specific-heat measurements were per-

TABLE I. Experimental parameters for $(Gd,Sm)M\mathrm{In}_5$, $(Gd,Sm)_2M\mathrm{In}_8$ (M=Rh or Ir), and $(Gd,Sm)\mathrm{In}_3$.

	a Å	c Å	T_N K	μ_{eff} μ_B	θ_p K
$GdIrIn_5$	4.622(4)	7.413(8)	42	7.9(1)	≈-64
Gd_2IrIn_8	4.615(4)	12.034(7)	41	8.2(1)	≈-75
$GdRhIn_5$	4.609(4)	7.444(7)	40	8.0(1)	≈-69
Gd_2RhIn_8	4.604(4)	12.060(9)	40	7.4(1)	-73
$SmIrIn_5$	4.634(4)	7.446(7)	14.3		
Sm_2IrIn_8	4.626(4)	12.088(7)	14.2		
$SmRhIn_5$	4.618(4)	7.470(8)	15.0		
Sm_2RhIn_8	4.621(4)	12.106(9)	15.0		
$LaIrIn_5$	4.710(4)	7.625(6)			
La_2IrIn_8	4.703(4)	12.314(7)			
$LaRhIn_5$	4.672(4)	7.602(7)			
La_2RhIn_8	4.699(4)	12.336(7)			
$GdIn_3$	4.6068[a]		≈45[a]	8.2[a]	≈-85[a]
$SmIn_3$	4.6265[a]		≈16[a]		

[a]See Ref. 7.

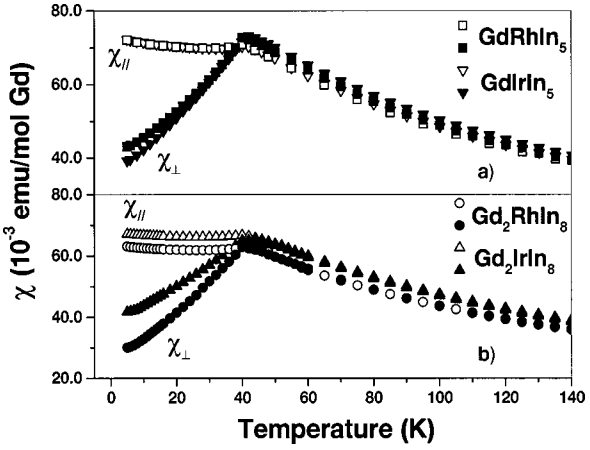

FIG. 1. Temperature dependence of the magnetic susceptibility, for applied field H along the c axis, $\chi_{\|}$ (open symbols), and in the ab plane, $\chi_{\perp}$ (solid symbols), for Gd_mMIn_{3m+2} (M=Rh or Ir) materials (a) for $m=1$ and (b) for $m=2$. The μ_{eff} and θ_p, obtained from Curie-Weiss law fitting for $T>150$ K are given in Table I.

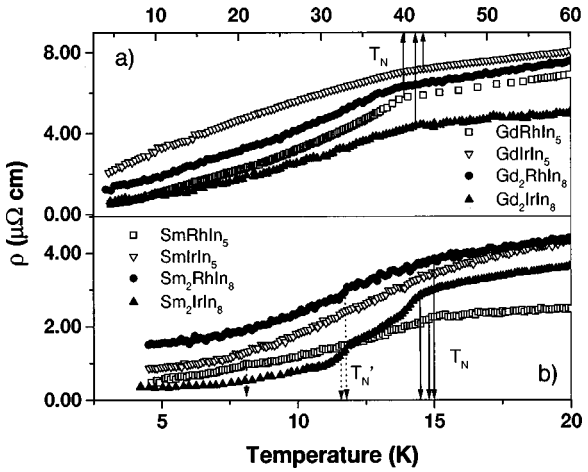

FIG. 3. Temperature dependence of the electrical resistivity for $(Gd,Sm)MIn_5$ and $(Gd,Sm)_2MIn_8$ (M=Rh or Ir) single crystals. The solid arrows point out the Néel temperatures for the compounds while the dashed arrows mark possible extra features below T_N.

formed in a small-mass calorimeter that employs a quasi-adiabatic thermal relaxation technique.[8] Samples used here ranged from 10 to 30 mg. Magnetization measurements were made in a Quantum Design dc superconducting quantum interference device and electrical resistivity was measured using a low-frequency ac resistance bridge and four-contact configuration.

III. RESULTS

Figures 1 and 2 present the temperature dependence of the magnetic susceptibility, for an applied field H along the c axis, $\chi_{\|}$, and in the ab plane, $\chi_{\perp}$, for the Gd_mMIn_{3m+2} and Sm_mMIn_{3m+2} materials, respectively. Each shows antiferromagnetic order, with $T_N<45$ K. For the Gd-based materials the magnetic susceptibility is significantly anisotropic only below T_N showing a typical anisotropy of an antiferromagnet with an easy axis in the plane. The effective magnetic moment (μ_{eff}) and the paramagnetic Curie-Weiss temperatures (θ_p) obtained from Curie-Weiss law fits for $T>150$ K for the Gd-based compounds are given in Table I. In the Sm-based case, the high-temperature magnetic anisotropy is probably associated with CEF in both ground $J=5/2$ and excited $J=7/2$ multiplet states of the Sm^{3+} ion.[9,10] As typical in Sm-based materials, the high-T behavior of the inverse of magnetic susceptibility does not show a linear temperature dependence due to a Van Vleck contribution (which complicates the extraction of μ_{eff} and θ_p from the data).[9,10]

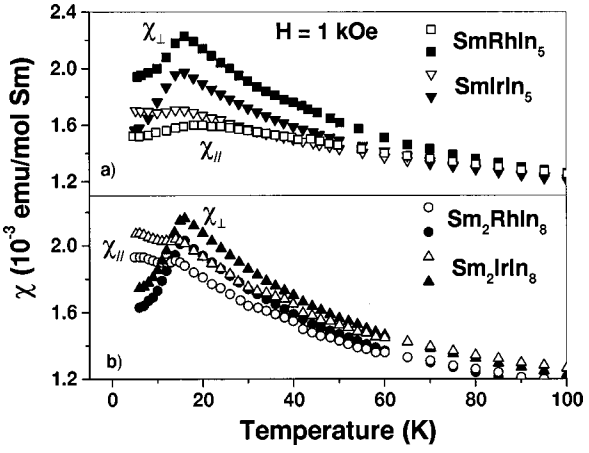

FIG. 2. Temperature dependence of the magnetic susceptibility, for applied field H along the c axis, $\chi_{\|}$ (open symbols), and in the ab plane, $\chi_{\perp}$ (solid symbols), for Sm_mMIn_{3m+2} (M=Rh or Ir) materials (a) for $m=1$ and (b) for $m=2$.

The temperature dependence of the electrical resistivity for $(Gd,Sm)MIn_5$ and $(Gd,Sm)_2MIn_8$ (M=Rh or Ir) single crystals is plotted in Fig. 3. The room-temperature value of the electrical resistivity varies between 20 and 30 $\mu\Omega$ cm and the high-temperature data show a metallic behavior for these compounds. At low temperatures, clear features can be seen at the respective ordering temperatures for all compounds. For the Sm-based homologues extra features also may be present in the data for $T<T_N$ for some of the compounds.

Figure 4 shows the specific heat divided by temperature (a) and the corresponding magnetic entropy (b) in the temperature range $2\lesssim T\lesssim 20$ K, for $SmMIn_5$ and Sm_2MIn_8 (M=Rh or Ir).

To calculate the magnetic entropy, the phonon contribution was estimated from the specific-heat data of $LaMIn_5$ (Refs. 1 and 2) and La_2MIn_8 (Ref. 3) (M=Rh or Ir) and subtracted from the total specific heat of the magnetic compounds. The main peaks in C/T corresponding to the onset of antiferromagnetic order can be seen at $T_N=14.18$ and 14.30 K for Sm_2IrIn_8 and $SmIrIn_5$, respectively, and at 15.00 K for both $SmRhIn_5$ and Sm_2RhIn_8 [Fig. 4(a)].

The Néel temperatures obtained from the specific-heat data are in very good agreement with the temperatures where the maximum in the magnetic susceptibility occurs (see Fig. 2).

For the Sm_2IrIn_8, the antiferromagnetic transition at 14.18 was found to be a first order transition with a latent heat of $\sim$10 J/mol. However, no hysteresis was observed in the re-

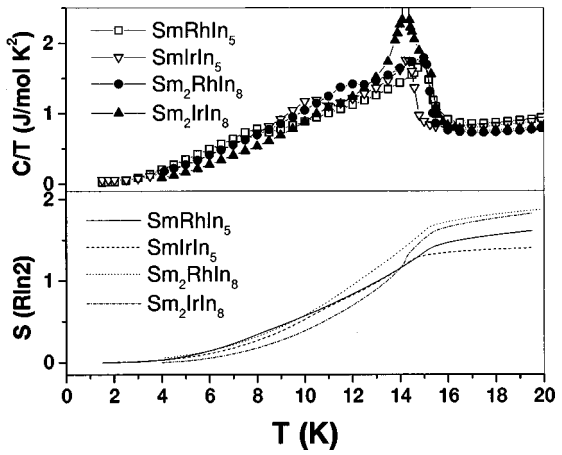

FIG. 4. Specific-heat data divided by temperature (a) and the corresponding magnetic entropy (b) in the temperature range $2 \lesssim T \lesssim 20$ K for SmMIn$_5$ and Sm$_2M$In$_8$ (M=Rh or Ir).

sistivity or magnetic susceptibility measurements as a function of temperature. The magnetic entropy recovered by T_N ranges between 1.4 and $1.8R \ln 2$ [Fig. 4(b)], suggesting that the magnetic order develops in a crystal-field doublet ground state with a nearby doublet excited state. Below T_N, a secondary feature in C_m/T was observed at 11.5, 10.0, 8.0, and 12.0 K for Sm_2IrIn_8, $SmIrIn_5$, $SmRhIn_5$, and Sm_2RhIn_8, respectively [Fig. 4(a)]. These secondary peaks are coincident with features in the resistivity for some of the compounds (see Fig. 3). Similar extra transitions below T_N also have been reported for $SmIn_3$ and they have been interpreted as successive magnetic transitions associated with quadrupolar ordering.[11]

IV. DISCUSSION

The cubic compounds RIn$_3$ are antiferromagnets with $T_N \lesssim 50$ K (Ref. 9) and their T_N and θ_p values follow de Gennes scaling quite well, with the exception of $CeIn_3$.[9] $NdIn_3$ and $SmIn_3$, whose magnetic order develops in a Γ_8 quartet crystal-field ground state, present additional magnetic transitions below T_N.[11–13] These complex magnetic states with successive magnet ordering arise due to the presence of magnetoelastic effects and both bilinear and quadrupolar exchange interactions.[11–13]

Surprisingly, the insertion of m MIn$_2$ layers along the c axis in (Gd,Sm)MIn$_5$ and (Gd,Sm)$_2M$In$_8$ (M=Rh or Ir) causes no significant changes in their Néel temperatures, whereas T_N shows a strong variation among the Ce- and Nd-based homologous.[3,5] It has been reported that the magnetization easy axis for (Ce,Nd)MIn$_5$ and (Ce,Nd)$_2M$In$_8$ (M=Rh or Ir) is along the c axis,[3,5] while the present data (see Figs. 1 and 2) suggest an easy axis in the ab plane for the (Gd,Sm)MIn$_5$ and (Gd,Sm)$_2M$In$_8$ (M=Rh or Ir) compounds. As we discuss below, this change in the direction of the magnetic easy axis may be related to a reduction through the rare earths in the competing anisotropic magnetocrystalline and crystal-field effects reported for Ce and Nd.[3,5]

In order to discuss the evolution of the magnetic properties of the RMIn$_5$ and R_2MIn$_8$ (M=Rh or Ir), we plot the

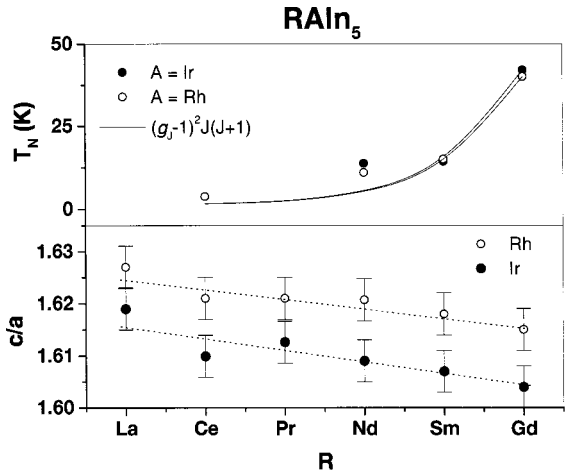

FIG. 5. T_N and c/a values plotted through the rare-earth series for the RMIn$_5$ (M=Rh or Ir) compounds. The solid lines are the de Gennes factor $[(g_J^2-1)][J(J+1)]$ for ground-state multiplet J of the rare earths normalized by the GdMIn$_5$ (M=Rh or Ir) T_N values and the dashed lines are a guide for the eye.

T_N and c/a ratio (see also Table I) for RMIn$_5$ (R=Ce,Nd,Sm,Gd; M=Rh,Ir) and R_2MIn$_8$ (R=Ce,Nd,Sm,Gd; M=Rh or Ir) in Figs. 5 and 6, respectively. Figure 7 shows the evolution of the Néel temperature for the homologous RMIn$_5$ and R_2MIn$_8$ (R=Ce,Nd,Gd,Sm; M=Rh or Ir) compounds compared to the their cubic RIn$_3$ (Ce,Nd,Sm,Gd) relatives.

The solid lines in Figs. 5 and 6 are the de Gennes factor $(g_J^2-1)[J(J+1)]$ for ground-state multiplet J through the rare earths. If one normalizes the de Gennes line to the Gd$_m M$In$_{3m+2}$ (M=Rh or Ir, m=1,2) T_N values, the Sm-based T_N values sit on the line but the T_N values for the Nd-based and the magnetic Ce-based compounds are above the line (see Figs. 5 and 6). In addition, the evolution of the Néel temperature for the homologous RMIn$_5$ and R_2MIn$_8$ compounds compared to their cubic RIn$_3$ relatives, varies by

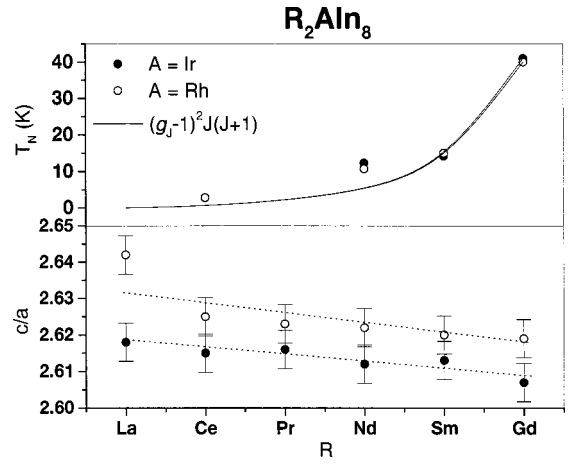

FIG. 6. T_N and c/a values plotted through the rare-earth series for the R_2MIn$_8$ (M=Rh or Ir) compounds. The solid lines are the de Gennes factor $[(g_J^2-1)][J(J+1)]$ for ground-state multiplet J of the rare earths normalized by the Gd$_2M$In$_8$ (M=Rh or Ir) T_N values and the dashed lines are a guide for the eye.

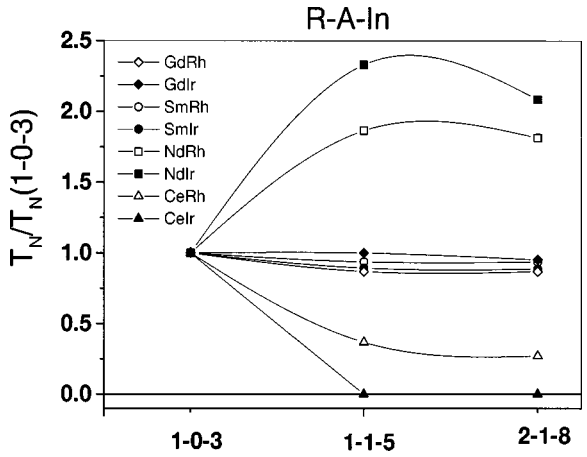

FIG. 7. Evolution of the normalized Néel temperatures for the Gd- and Sm-based compounds. For comparison, data for the homologous Ce- and Nd-based compounds and for cubic $R\mathrm{In}_3$ (R = Ce,Nd,Sm,Gd), are also shown.

less than 10% for R=Gd and Sm while T_N is raised by a factor of 2 for the Nd-based tetragonal variants and is suppressed completely (M=Ir) or to less than 0.5 of the CeIn_3 value (M=Rh) for the Ce-based homologous compounds (see Fig. 7).[3,5]

De Gennes scaling[14] does not take into account CEF, Kondo effects, and/or spatial dependence and anisotropic effects in the effective exchange parameter. Some of these effects are clearly present in the Ce-based and Nd-based homologues.[1,3,5] Therefore it is not a surprise that the T_N values for the Ce-based and Nd-based homologues do not follow a de Gennes scaling. Furthermore, our data for Gd- and Sm-based compounds suggest that anisotropic and/or CEF effects may decrease along the rare-earth series. The Sm-based compounds (Sm^{3+} has $J=5/2$, identical to Ce^{3+}) show smaller ratios $\chi_{easy}/\chi_{\perp easy}$ ranging between 1.05 and 1.30 (see Fig. 2) while these ratios range from 1.20 to greater than 2 for the Ce-based analogues.[3] A possible explanation for this behavior may be related to the systematic decreasing of c/a ratio through the rare-earth series (see Figs. 5 and 6) which may diminish the tetragonal character of the crystal-electric field and/or the magnetic anisotropy effects in the Sm case. The Gd-based compounds, which are expected to present small CEF due to the S character of the Gd^{3+} ($S=7/2$, $L=0$) ion, show only slight anisotropy in the magnetic susceptibility above T_N (see Fig. 1) and also small T_N evolution within the $R_mM_n\mathrm{In}_{3m+2n}$ (M=Rh or Ir, m=1,2; n=0,1) compounds. Therefore the absence or reduction of Kondo, CEF effects and/or magnetic anisotropy for the $(\mathrm{Gd,Sm})M\mathrm{In}_5$ and $(\mathrm{Gd,Sm})_2M\mathrm{In}_8$ (M=Rh or Ir) compounds may cause their magnetic properties to be roughly the same as their cubic relatives GdIn_3 and SmIn_3. Further investigation in the evolution of the crystal-field parameters and the character of the magnetic state for $RM\mathrm{In}_5$ and $R_2M\mathrm{In}_8$ including heaviest rare earths (e.g., R=Dy, Er, or Yb) would be valuable in confirming our supposition.

V. CONCLUSIONS

We have reported a new series of Gd- and Sm-based antiferromagnetic ($T_N<45$ K) compounds. Their low-temperature magnetic properties remain similar to their SmIn_3 and GdIn_3 cubic relatives. Comparisons among the present data and the magnetic properties of isostructural (Ce,Nd) $(\mathrm{Rh,Ir})\mathrm{In}_5$ and $(\mathrm{Ce,Nd})_2(\mathrm{Rh,Ir})\mathrm{In}_8$ and of de Gennes scaling as a function of rare earth in a given structure suggest that the reduction CEF effects and related magnetic anisotropy through the rare-earth series for the tetragonal variants may cause the magnetic properties of $(\mathrm{Gd,Sm})M\mathrm{In}_5$ $(\mathrm{Gd,Sm})_2M\mathrm{In}_8$ (M=Rh or Ir) and their cubic relatives GdIn_3 and SmIn_3 to be nearly the same.

ACKNOWLEDGMENTS

We thank S. B. Oseroff for helpful discussions. Work at Los Alamos is performed under the auspices of the U.S. Dept. of Energy. P. G. Pagliuso also thanks FAPESP (SP-Brazil) Grant No. 99/01062-0.

*Permanent address: Florida State University, Tallahassee, FL 32306

[1] H. Hegger, C. Petrovic, E.G. Moshopoulou, M.F. Hundley, J.L. Sarrao, Z. Fisk, and J.D. Thompson, Phys. Rev. Lett. **84**, 4986 (2000).

[2] C. Petrovic, R. Movshovich, M. Jaime, M.F. Hundley, J.L. Sarrao, P.G. Pagliuso, Z. Fisk, and J.D. Thompson, Europhys. Lett. (to be published).

[3] J.D. Thompson, R. Movshovich, Z. Fisk, F. Bouquet, N.J. Curro, R.A. Fisher, P.C. Hammel, H. Hegger, M.F. Hundley, M. Jaime, P.G. Pagliuso, C. Petrovic, N.E. Phillips, and J.L. Sarrao, J. Magn. Magn. Mater. (to be published).

[4] E.G. Moshopoulou, Z. Fisk, J.L. Sarrao, and J.D. Thompson, J. Solid State Chem. (to be published).

[5] P.G. Pagliuso, J.D. Thompson, M.F. Hundley, and J.L. Sarrao, Phys. Rev. B **62**, 12 266 (2000).

[6] Pagliuso *et al.* (unpublished).

[7] Ya.M. Kalychak, J. Alloys Compd. **291**, 80 (1999).

[8] R. Bachmann, F.J. DiSalvo, T.H. Geballe, R.L. Greene, R.E. Howard, C.N. King, H.C. Kivisch, K.N. Lee, R.E. Schwall, H.V. Thomas, and R.B. Zubek, Rev. Sci. Instrum. **43**, 205 (1972).

[9] K.H.J. Buschov, H.W. de Wijn, and M. Van Diepen, J. Chem. Phys. **50**, 137 (1969).

[10] T. Tsuchida and W.E. Wallace, J. Chem. Phys. **43**, 3811 (1965).

[11] M. Kasaya, B. Liu, M. Sera, T. Kasuya, D. Endoh, T. Goto, and F. Fujimura, J. Magn. Magn. Mater. **52**, 289 (1985).

[12] M. Amara, R.M. Galéra, P. Morin, T. Verez, and P. Burlet, J. Magn. Magn. Mater. **130**, 127 (1994); M. Amara, R.M. Galéra, P. Morin, J. Voiron, and P. Burlet, *ibid.* **131**, 402 (1994); M. Amara, R.M. Galéra, P. Morin, J. Voiron, and P. Burlet, *ibid.* **140**, 1157 (1994).

[13] A. Czopnik, J. Kowalewski, and M. Hackemer, Phys. Status Solidi A **127**, 243 (1991).

[14] P.G. De Gennes, Compt. Rend. **247**, (1958); P.G. De Gennes, J. Phys. Radium **23**, 510 (1962); B. Coqblin, *The Electronic Structure of Rare-Earth Metal and Alloys: The Magnetic Heavy Rare Earths* (Academic Press, New York, 1977).